

Zitterbewegung effect in spin-1 ultracold atoms

Yi-Cai Zhang¹, Song-Wei Song¹, Chao-Fei Liu^{1,2} and W. M. Liu¹

¹*Beijing National Laboratory for Condensed Matter Physics,*

Institute of Physics, Chinese Academy of Sciences, Beijing 100190, China

²*School of Science, Jiangxi University of Science and Technology, Ganzhou 341000, China*

(Dated: June 5, 2019)

The Zitterbewegung-like effect in spin-1 cold atoms is investigated in the presence of the Zeeman field and external parabolic trap. It is shown that the Zeeman field and parabolic trap have significant effect on the Zitterbewegung oscillatory behaviors. Multi-frequency Zitterbewegung oscillation can be induced by the applied Zeeman field in comparison to that in two components atoms. In addition, a much slowly damping Zitterbewegung oscillation can be achieved by adjusting the linear and quadratic zeeman parameters properly, which is favorable to the observation of Zitterbewegung oscillation in the experiments. In the presence of the harmonic trap, the subpackets corresponding to different eigenenergies would always keep coherent, resulting in persistent Zitterbewegung oscillations. If the initial condition of Gaussian packet is prepared, the Zitterbewegung oscillation would display very complicated and irregular oscillation characteristics due to coexistence of different frequencies of the Zitterbewegung oscillation.

PACS numbers: 03.75.Hh, 03.75.Nt, 05.30.Jp, 03.65.Ge

I. INTRODUCTION

The Zitterbewegung (ZB) effect, which is characterized by high frequency oscillations (trembling motion) for Dirac electrons was firstly predicted by Schrödinger [1]. The ZB effect is purely a relativistic phenomenon and originates from the interference between the positive and negative energy states of the electron. The experimental observation of the electron ZB has not been realized due to its high frequency (the order of $\hbar\omega = 2m_e c^2 \sim 1\text{MeV}$) and small oscillatory amplitude (the order of Compton wavelength of electron $\hbar/m_e c \sim 10^{-12}m$). However, it is shown that there exist ZB-like effects in condensed matter systems [2], graphene [3–6], superconductors [7], topological insulators, photonic crystal [8, 9] and semiconductor quantum wells [10, 11]. Thence, the ZB-like effect has attracted great attentions recently, both theoretically and experimentally in various physics fields [12–17].

Because of the well controlled length and energy scales in cold atoms, it is possible to observe the ZB-like oscillation in cold atoms experiments. Recently, there were proposals to simulate the ZB effect by using ultracold atoms [18–22], wherein most authors focus on the ZB effect of two component atoms with spin-orbit coupling in the free space. Thus, the quasi-momenta is a good quantum number, the Hamiltonian can be diagonalized within the momentum space. By using the Gaussian packet as the initial state, it is shown that the oscillatory amplitude of ZB deceases with time and the ZB phenomenon has a transient characteristic. It would be of significance to find ways to stabilize and manipulate the ZB oscillation for potential applications.

As shown in Ref. [23], ZB-like phenomena are fairly common characteristics for multi-level systems. However, the multi-frequency ZB oscillation in ultracold atomic system has not been investigated to the best of our knowl-

edge. The effects which is induced by the external field and the trap on the ZB oscillations need to be clarified. In this paper, we will try to investigate the above concerns by using the external magnetic field and parabolic trap.

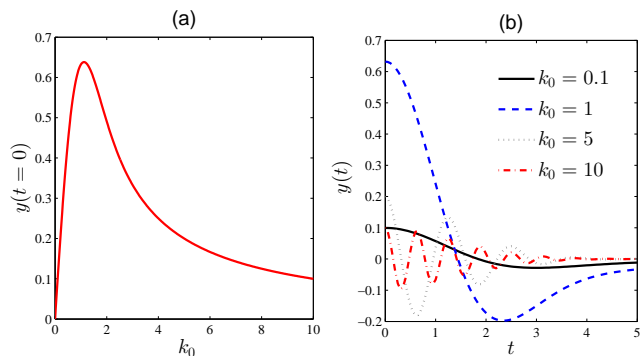


FIG. 1. (a): The maximum ZB oscillatory amplitude as a function of the central momentum with zero Zeeman field. The red line is obtained by exactly numerical integral. (b): The ZB oscillations with zero Zeeman field in the free space.

In the present paper, we investigate the characteristics of the multi-frequency oscillation induced by Zeeman field and the persistent oscillations in the presence of the external parabolic trap in the spin-1 ultra-cold atoms. In Sec. II, we introduce the general Hamiltonian of spin-1 atoms with spin-orbit coupling, and then focus on the ZB oscillatory characteristics in the Zeeman fields. In Sec. III, the ZB oscillatory characteristics in harmonic trap are investigated. A summary is presented in Sec. IV.

II. ZB EFFECT IN ZEEMAN FIELDS

The general Hamiltonian of the spin-orbit coupled spin-1 atoms in the presence of the external Zeeman field is

$$\begin{aligned}
 H &= T + V_{trap} + V_{SO} + V_Z \\
 T &= \frac{p_x^2 + p_y^2}{2m} \\
 V_{trap} &= \frac{m\omega^2(x^2 + y^2)}{2} \\
 V_{SO} &= \gamma p_x F_x + \gamma p_y F_y \\
 V_Z &= p F_z + q F_z^2,
 \end{aligned} \tag{1}$$

where T , V_{trap} , V_{SO} , V_Z are the kinetic energy, the harmonic potential, the spin-orbit coupling interaction and the Zeeman shift respectively. The spin-1 matrices are given by

$$F_x = \begin{pmatrix} 0 & \frac{1}{\sqrt{2}} & 0 \\ \frac{1}{\sqrt{2}} & 0 & \frac{1}{\sqrt{2}} \\ 0 & \frac{1}{\sqrt{2}} & 0 \end{pmatrix}, F_y = \begin{pmatrix} 0 & \frac{-i}{\sqrt{2}} & 0 \\ \frac{i}{\sqrt{2}} & 0 & \frac{-i}{\sqrt{2}} \\ 0 & \frac{i}{\sqrt{2}} & 0 \end{pmatrix}$$

$$F_z = \begin{pmatrix} 1 & 0 & 0 \\ 0 & 0 & 0 \\ 0 & 0 & -1 \end{pmatrix}.$$

Without the external parabolic trap, the Hamiltonian can be diagonalized in the momentum space as

$$H' = U^+ H U = \begin{pmatrix} \omega_1 & 0 & 0 \\ 0 & \omega_2 & 0 \\ 0 & 0 & \omega_3 \end{pmatrix}, \tag{2}$$

where $\omega_1 = (p_x^2 + p_y^2)/2m + n \cos u - b/3$, $\omega_2 = (p_x^2 + p_y^2)/2m + n \cos(u + 4\pi/3) - b/3$, $\omega_3 = (p_x^2 + p_y^2)/2m + n \cos(u + 2\pi/3) - b/3$ are roots of eigen-equation $\text{Det}(\omega I - H) = 0$. The corresponding eigenvectors are

$$|\alpha_i\rangle = \frac{1}{n_i} \begin{pmatrix} -(p_x^2 + p_y^2) + 2\omega_i(p - q + \omega_i) \\ \sqrt{2}(p - q + \omega_i)(p_x + ip_y) \\ (p_x + ip_y)^2 \end{pmatrix}, \tag{3}$$

where n_i is normalization coefficient, $n = \sqrt{-4p_1/3}$, $u = \arccos(-q_1(-p_1/3)^{-3/2}/2)/3$, $p_1 = c - b^2/3$, $q_1 = d - bc/3 + 2b^3/27$, $b = -2q$, $c = -(p_x^2 + p_y^2) + q^2 - p^2$, $d = (p_x^2 + p_y^2)q$, respectively. In general, they are the functions of the momentum (p_x, p_y) and Zeeman shift parameter (p, q) .

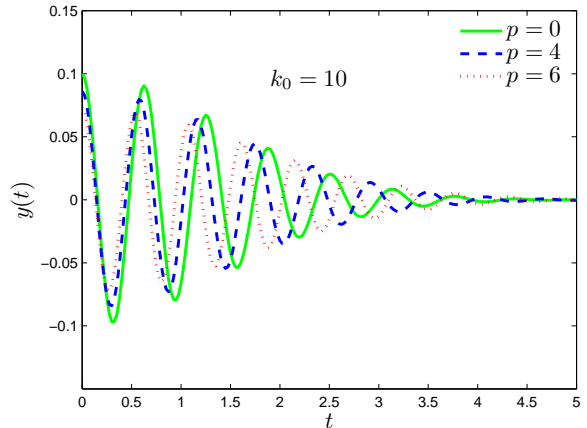


FIG. 2. ZB oscillation in spin-1 atoms with only linear Zeeman field. The green line denote the ZB with zero Zeeman field. The blue, red lines are ZB with a linear Zeeman field $p=4$ and $p=6$ respectively.

The position operator in the Heisenberg picture is [23]

$$\vec{r}(t) = \vec{r}(0) + \sum_k Z_{k;k} + t \sum_k \vec{V}_k Q_k + \sum_{k,l \neq m} e^{i\omega_{kl}t} \vec{Z}_{k;l}, \tag{4}$$

where $\vec{V}_k = \frac{\partial \omega_k}{\partial \vec{p}}$, $Q_k = |\alpha_k\rangle\langle\alpha_k|$ are the group velocity and the projection operator, respectively. k, l denote the energy branch $\omega_1, \omega_2, \omega_3$ and $\omega_{kl} = \omega_k - \omega_l$ is the eigen-energy difference. $Z_{k;l} = iQ_k \frac{\partial Q_l}{\partial \vec{p}}$ is the so-called *Zitterbewegung amplitudes* (see Ref. [23]). The first and second terms are constants in Eq. (4). The third term is the uniform motion and the fourth corresponds to the ZB oscillation. As shown in the fourth term, the position operator usually undergoes oscillatory behaviors with multi-frequencies. We will calculate the average value of position by using an initial wave function of Gaussian density distribution:

$$|g\rangle = \frac{1}{\sqrt{\pi\delta^2}} e^{-\frac{x^2+y^2}{2\delta^2}} e^{ik_0x} \begin{pmatrix} 1 \\ 0 \\ 0 \end{pmatrix} \tag{5}$$

The wave function expressed in momentum space is

$$|g\rangle = \sqrt{\frac{\delta^2}{\pi}} e^{-\frac{1}{2}\delta^2[(p_x - k_0)^2 + p_y^2]} \begin{pmatrix} 1 \\ 0 \\ 0 \end{pmatrix}, \tag{6}$$

where δ and k_0 are the width and the average momentum of the wave packet. The mean value of position is $\langle \vec{r}(t) \rangle = \langle g | \vec{r}(t) | g \rangle$.

From Eq. (1) and (4), we can find that the kinetic energy of Hamiltonian does not contribute to the ZB oscillation. Therefore, during the discussion of the ZB, the

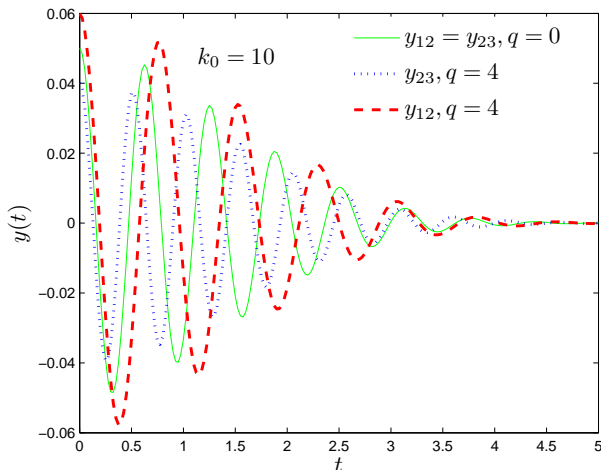


FIG. 3. ZB oscillation with only quadratic Zeeman field. The blue and red ones are ZB oscillations corresponding to ω_{23} and ω_{12} for a quadratic Zeeman field $q=4$. For the sake of comparison the green line corresponding to the case of zero Zeeman field is also plotted.

kinetic energy part is neglected. In this section, we take the reduced Planck constant \hbar , the spin-orbit coupling γ and wave packet width δ as independent fundamental units. The other derived physical quantities, such as time, momentum, energy are measured by δ/γ , \hbar/δ and $\gamma\hbar/\delta$, respectively.

We explore the following four cases according to the applied Zeeman field.

Case 1: $p = 0$ and $q = 0$

Considering the initial wave packet (5), only the matrix element of $(y(t))_{1,1}$ has contribution to the oscillation part of the mean value of y component of position operator. In the Heisenberg picture, it takes the form,

$$y(t)_{1,1} = \frac{p_x}{p_x^2 + p_y^2} \cos(\gamma t \sqrt{p_x^2 + p_y^2}). \quad (7)$$

Substituting the initial state, we calculate the mean value of the oscillatory part of y

$$\begin{aligned} \langle y(t) \rangle &= \int_{-\infty}^{\infty} \int_{-\infty}^{\infty} d\vec{p} \frac{\delta^2 p_x \cos(\gamma t \sqrt{p_x^2 + p_y^2}) e^{-\delta^2((p_x - k_0)^2 + p_y^2)}}{p_x^2 + p_y^2} \\ &= 2\delta e^{-\delta^2 k_0^2} \text{Re} \left[\int_0^{\infty} d\rho e^{-\rho^2 + i \frac{\gamma t}{\delta} \rho} I_1(2\delta k_0 \rho) \right], \end{aligned} \quad (8)$$

where $\rho = \delta \sqrt{p_x^2 + p_y^2}$ and $I_1(x)$ are dimensionless variable of integration and the modified Bessel function of first order, respectively. In order to capture qualitative behaviors of ZB oscillation, we assume $\delta k_0 \gg 1$, and the asymptotic formula $I_1(x) \approx e^x / \sqrt{2\pi x}$ can be used as done in Ref. [27]. The integral

$\int_0^{\infty} d\rho e^{(-\rho^2 + i \frac{\gamma t}{\delta} \rho + 2\delta k_0 \rho)} / \sqrt{2\delta k_0 \rho}$ can be evaluated using the method of steepest descents

$$\langle y(t) \rangle \approx \frac{\delta e^{-\frac{\gamma^2 t^2}{4\delta^2}}}{(\delta^4 k_0^4 + \frac{k_0^2 \gamma^2 t^2}{4})^{\frac{1}{4}}} \cos(\gamma k_0 t - \frac{\theta}{2}), \quad (9)$$

where $\theta = \arctan(\frac{\gamma t}{2\delta^2 k_0})$.

From Eq. (9), it is shown that in the case of $\delta k_0 \gg 1$, the average position along the perpendicular direction of non-vanishing average momentum k_0 undergoes a damping oscillation with a single frequency. There are two factors which result in the damping. One is the exponentially decreasing term $e^{-\frac{\gamma^2 t^2}{4\delta^2}}$ which originates from the increasing spatial separation between the subpackets corresponding to the higher and lower eigenenergy branches [3]. Because the overlap between the subpackets gets smaller and smaller with time, the oscillatory amplitude gets smaller and smaller. We can identify the non-vanishing relative group velocity between the subpackets corresponding to different energy branches at the average momentum $v = \partial_{p_x} \omega_{12}|_{k_0} = \gamma$. It is anticipated that, when the relative group velocity gets smaller, the damping would be suppressed. The other one is the term $1/(\delta^4 k_0^4 + \frac{k_0^2 \gamma^2 t^2}{4})^{\frac{1}{4}}$, which results in a much slower damping compared with the exponentially decreasing term. In the case of $\delta k_0 \gg 1$, the exponentially decreasing term dominates the whole damping trend before the disappearing of the ZB.

For the limit of $\delta k_0 \ll 1$, the modified Bessel function can be expanded as Taylor series $I_1(x) = \frac{x}{2} + \frac{x^3}{16} + \frac{x^5}{384} + O(x^7)$. By Keeping only the first linear term, we get

$$\begin{aligned} \langle y(t) \rangle &\approx 2\delta^2 k_0 e^{-\delta^2 k_0^2} \int_0^{\infty} d\rho e^{-\rho^2} \rho \cos(\frac{\gamma t \rho}{\delta}) \\ &= \delta^2 k_0 e^{-\delta^2 k_0^2} (1 - \frac{\gamma t}{\delta} D(\frac{\gamma t}{2\delta})), \end{aligned} \quad (10)$$

where $D(x) = \frac{1}{2} \int_0^{\infty} e^{-t^2/4} \text{sin}(xt) dt$ is the Dawson function.

We can see from Eq. (10) that there will be no integrate ZB oscillation when the average momentum is very small (see also panel (b) in Fig.1). We notice that a similar result is found in 4×4 Luttiger Hamiltonian by Demikhovskii, *et al* [35].

From the above approximate formulas, the maxima of the ZB oscillatory amplitude $y(t = 0)$ can be obtained for the two limit case. In the case of the average momentum $k_0 \ll 1$, it is proportional to the average momentum. When $k_0 \gg 1$, the ZB amplitude is inversely proportional to the average momentum. We numerically investigate the maximum amplitude as a function of the average momentum in Fig.1. In panel (a) of Fig.1, there exists a maxima of oscillatory amplitude. The maximum value occur at around $k_0 \sim 1$.

Case 2: $p \neq 0$ and $q = 0$

The oscillatory part of $y(t)$ in the Heisenberg picture

is

$$(y(t))_{1,1} = \frac{p_x}{p_x^2 + p_y^2 + p^2} \cos(\gamma t \sqrt{p_x^2 + p_y^2 + p^2}). \quad (11)$$

In principle, one could be able to get the asymptotic results similar to the former calculations. However the result is so complicated that we could not get clear physical meaning from its expression. Inspired by the case of zero Zeeman field, we will give approximate expression to fit the data obtained from the exact numerical integral under conditions of $\delta k_0 \gg 1$. The approximate formula is

$$\begin{aligned} \langle y(t) \rangle &= \langle g|y(t)|g \rangle \\ &= 2\delta^2 e^{-\delta^2 k_0^2} \text{Re} \left[\int_0^\infty d\rho \frac{\rho^2 e^{-\delta^2 \rho^2 + I\gamma t \sqrt{\rho^2 + p^2}}}{\rho^2 + p^2} I_1(2\delta^2 k_0 \rho) \right] \\ &\approx \frac{k_0^2}{k_0^2 + p^2} \frac{\delta e^{-\frac{v_{12}^2 t^2}{4\delta^2}}}{(\delta^4 k_0^4 + \frac{k_0^2 v_{12}^2 t^2}{4})^{\frac{1}{4}}} \cos(\omega_{12} t), \end{aligned} \quad (12)$$

where $v_{12} = \partial_{p_x} \omega_{12}|_{k_0} = \frac{rk_0}{\sqrt{k_0^2 + p^2}}$ is the relative group velocity at the average momentum and $\omega_{12} = \gamma \sqrt{k_0^2 + p^2}$ is the energy difference between different energy branches at the central momentum. We can see from Eq. (12) that the amplitude is suppressed by the applied linear Zeeman field. With the increase of the linear Zeeman field, the decaying trend is suppressed. The reason is that with the increase of linear Zeeman field, the relative velocity between sub-packets corresponding to different energy branches at the average momentum $v_{12} = \frac{\gamma k_0}{\sqrt{k_0^2 + p^2}}$ gets smaller. Then, the sustained coherence between sub-packets lead to the suppression of decaying. For specific parameters, we depict the ZB oscillations with only the linear Zeeman field in Fig.2.

Case 3: $p = 0$ and $q \neq 0$

The oscillation part of the component $y(t)_{1,1}$ of the position operator in the Heisenberg picture is

$$y(t)_{1,1} = \frac{p_x \omega_{23} \cos(t\omega_{12})}{2\omega_{13}(p_x^2 + p_y^2)} + \frac{p_x \omega_{12} \cos(t\omega_{23})}{2\omega_{13}(p_x^2 + p_y^2)}, \quad (13)$$

where $\omega_{23} = \frac{1}{2}(q + \sqrt{4(p_x^2 + p_y^2) + q^2})$, $\omega_{12} = \frac{1}{2}(-q + \sqrt{4(p_x^2 + p_y^2) + q^2})$, $\omega_{13} = \sqrt{4(p_x^2 + p_y^2) + q^2}$.

By using the similar approximation, the average position along y direction is approximated by

$$\begin{aligned} \langle y(t) \rangle &= \langle g|y(t)|g \rangle \\ &= y_{12} + y_{23} \\ &\approx \frac{\omega_{2,3}(k_0)}{2\omega_{13}} \frac{\delta e^{-\frac{v_{12}^2 t^2}{4\delta^2}}}{(\delta^4 k_0^4 + \frac{k_0^2 v_{12}^2 t^2}{4})^{\frac{1}{4}}} \cos(\omega_{12} t) \\ &+ \frac{\omega_{12}(k_0)}{2\omega_{13}} \frac{\delta e^{-\frac{v_{23}^2 t^2}{4\delta^2}}}{(\delta^4 k_0^4 + \frac{k_0^2 v_{23}^2 t^2}{4})^{\frac{1}{4}}} \cos(\omega_{23} t), \end{aligned} \quad (14)$$

where y_{ij} is the ZB oscillation with frequency which is energy difference between the energy branches i and j at the average momentum. $v_{12} = \partial_{p_x} \omega_{12}|_{k=k_0} = \frac{rk_0}{\sqrt{k_0^2 + p^2}}$, $v_{23} = \partial_{p_x} \omega_{23}|_{k=k_0} = \frac{rk_0}{\sqrt{k_0^2 + q^2}}$ are relative group velocity between different energy branches at the central momentum.

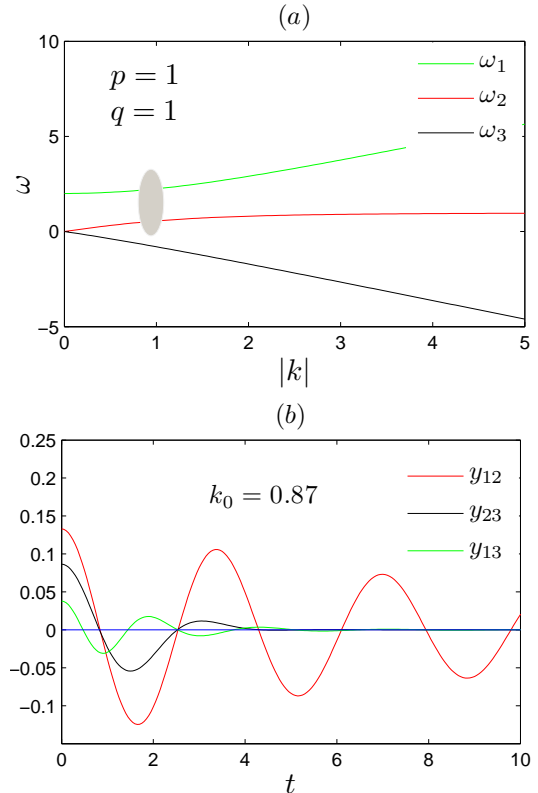


FIG. 4. (a): The energy spectrum with both linear and quadratic Zeeman field ($p=1, q=1$). The green (red, black) lines denote the three energy branches ω_1 , ω_2 and ω_3 , respectively. The grey ellipse region is where the relative group velocity v_{12} approaches zero. (b): The ZB oscillations for the specific average momentum $k_0 = 0.87$. The red, black and green lines denote the ZB oscillations with the frequency corresponding to ω_{12} , ω_{23} and ω_{13} respectively.

In the presence of only the quadratic zeeman filed, the ZB oscillation split into two oscillations with different amplitudes and frequencies (see Fig. 3). The amplitude of ZB oscillation with higher frequency is smaller. Because of the equal relative group velocity at the central momentum $v_{12} = v_{23}$, the two ZB oscillations have the same exponential decreasing factor and the damping trends for the two ZB oscillations are the same on the whole. With the increase of the quadratic Zeeman field, the split of both the amplitudes and frequencies of the two ZB gets more evident.

Case 4: $p \neq 0$ and $q \neq 0$

In the presence of both the linear and quadratic zeeman field, the analytical expression of the position op-

erator in the Heisenberg picture is quite complicated. We depict the ZB oscillations with $p = 1$, $q = 1$ and $k_0 = 0.87$ in Fig.4. We can see that there are usually three frequencies when both the linear and quadratic Zeeman field exist. We find that when the relative group velocity $v_{ij} = \partial_{p_x} \omega_{ij}$ between different eigen-states at the central momentum approaches zero, the mean position will damp much slowly. As shown in the bottom panel of Fig.4, when the central momentum is chosen near the elliptic region, the relative velocity between sub-packets nearly vanish, the ZB oscillation corresponding to ω_{12} display much slowly decaying trend. The slowly decaying amplitude would be favorable for the observation of ZB in experiments.

III. THE ZB EFFECT IN TRAPPED ATOMS

As shown in the above section, the oscillatory amplitude of ZB usually decays with time when the initial state is chosen as Gaussian packet with non-vanishing average momentum. In the trapped system, the oscillatory behaviors have unique characteristics compared with that in the free space. Firstly, due to the confinement of trap, the atoms could not escape from the trap. Hence, the subpackets corresponding to different eigenenergies would always keep coherent, resulting in non-decayed ZB oscillations. Secondly, due to the existence of infinite energy levels in the trap, the ZB oscillation shows very complicated features.

In this section, we adopt the natural units of harmonic oscillators. The length, mass and time are measured by $\sqrt{\hbar/m\omega}$, m and $1/\omega$ respectively. The other physical quantities, such as, energy, momentum, velocity are measured by $\hbar\omega$, $\sqrt{\hbar m\omega}$ and $\sqrt{\hbar\omega/m}$, respectively.

Similar to that in Ref. [23], we decompose the time evolution operator as $U = e^{-iHt} = \sum_l e^{-iE_l t} |l\rangle\langle l|$, where $|l\rangle$ is the eigenstates of Hamiltonian and E_l the corresponding eigenenergy. We generalize Eq. (3) to the trapped system and obtain the position operator in Heisenberg picture as

$$\vec{r}(t) = \vec{r}(0) + \sum_k Z_{k;k} + \sum_{k,l \neq k} e^{i\omega_{kl}t} \vec{Z}_{k;l}, \quad (15)$$

where $\vec{Z}_{k;l} = |k\rangle\langle k|\vec{r}|l\rangle\langle l|$ is the so-called ZB amplitude operator, and ω_{kl} is energy difference between eigenenergies. To calculate the average value of position operator, the eigenstates and eigenenergies are required. Before the numerical calculation of the eigen-equations, we will discuss the symmetries of Hamiltonian. The Hamiltonian have rotation symmetries along z axial direction. Thus the total angular momenta along z direction $J_z = L_z + F_z$ is a good quantum number. We will label the eigenstates and energies with good quantum number $j_z = m$. In the polar coordinates (ρ, θ) , the eigen-function can be written in the following form

$$|\psi_m(\rho, \theta)\rangle = \begin{pmatrix} \phi_1(\rho) \frac{e^{i(m-1)\theta}}{\sqrt{2\pi}} \\ \phi_0(\rho) \frac{e^{im\theta}}{\sqrt{2\pi}} \\ \phi_{-1}(\rho) \frac{e^{i(m+1)\theta}}{\sqrt{2\pi}} \end{pmatrix}, \quad (16)$$

with $j_z = m$.

In addition to the rotational symmetry, there is time reversal symmetry in the absence of the Zeeman field. The time reversal operator is expressed as $T = UK$ with $U = \exp(-i\pi F_y)$ and K the complex conjugate operation. Its matrix form is

$$T = \begin{pmatrix} 0 & 0 & 1 \\ 0 & -1 & 0 \\ 1 & 0 & 0 \end{pmatrix} K. \quad (17)$$

Then the time reversal state can be obtained as $|\psi_{-m}(\rho, \theta)\rangle = T|\psi_m(\rho, \theta)\rangle$ with degenerate eigenenergies $E_{-m,l} = E_{m,l}$. The eigenstates are doubly degenerate except for the states corresponding to $m = 0$.

We will work with the basis of 2D harmonic oscillator, and the basis can also be introduced by two independent operators in terms of operators of $a_x(y)$ [25]

$$\begin{aligned} a_d &= \frac{1}{\sqrt{2}}(a_x - ia_y) \\ a_g &= \frac{1}{\sqrt{2}}(a_x + ia_y), \end{aligned} \quad (18)$$

where $a_x(y)$ is annihilation operators of the $x(y)$ axial. The position and momentum operators can be expressed in terms of the operators in Eq.(18) and their corresponding adjoint operators. For example, the y component of the position is $y = \frac{i}{2}(a_d - a_d^\dagger - a_g + a_g^\dagger)$. The harmonic oscillator basis can be written as

$$|\chi_{n_d, n_g}\rangle = \frac{1}{\sqrt{(n_d)!(n_g)!}} (a_d^\dagger)^{n_d} (a_g^\dagger)^{n_g} |0, 0\rangle \quad (19)$$

with $|0, 0\rangle$ is the ground state of a 2D harmonic oscillator. The 2D harmonic oscillator basis can be expressed in the coordinate space as

$$\phi_{n,m}(\rho, \theta) = \langle \vec{r} | \chi_{n_d, n_g} \rangle = R_{n,m}(\rho) \frac{e^{im\theta}}{\sqrt{2\pi}}, \quad (20)$$

where $n = n_g$ and $m = n_d - n_g$, $R_{n,m}(\rho) = (-1)^n \sqrt{\frac{2(n!)}{(n+|m|)!}} \rho^{|m|} e^{-\rho^2/2} L_n^{|m|}(\rho^2)$, $L_n^{|m|}(x) = \sum_{k=0}^n C_{n+|m|}^{n-k} \frac{(-x)^k}{k!}$ is the associated Laguerre polynomial, $C_n^k = \frac{n!}{(n-k)!k!}$ is the binomial coefficient.

From the expression of the position operators in terms of $a_g(d)$ and their adjoint operators, there exist an important selection rule for ZB amplitude operators

$$\begin{aligned} \vec{Z}_{m,l;m',l'} &= |m,l\rangle\langle m,l|\vec{r}|m',l'\rangle\langle m',l'| = 0, \\ &\quad (m - m' \neq \pm 1), \end{aligned} \quad (21)$$

where l labels the eigenstates belonging to the same quantum m . It is shown that only for $m = m' \pm 1$, there exist non-vanishing *ZB amplitude*. From the above equation, it is found that the second term in Eq. (15) vanishes, i.e. $\vec{Z}_{k;k} = \vec{Z}_{m,l;m,l} = 0$.

One can express the Hamiltonian in the form of matrix by adopting the basis of the harmonic oscillator in Eq. (19). The corresponding eigenenergies and eigenstates can be obtained through direct numerical diagonalization [24].

Now we investigate the ZB oscillatory characteristics in the trap. First of all, when the the initial state is the superposition of two eigenstates, there would be a oscillation with one single frequency which is the difference of two eigen-energies shown by equation (15). The oscillatory amplitude does not decay. This is because that the components corresponding to two eigenenergies in the initial state always keep coherent as stated before.

Then, we calculated the ZB oscillations when an initial Gaussian wave packet with non-vanishing average momentum is used. The projections of the initial state on the harmonic basis are required in the calculation the average value of the position. The detailed calculations of the projection are listed in the appendix. From Eq. (15), we find that the number of the oscillatory frequencies involved in ZB oscillation is usually arbitrary when the initial state is chose in a completely arbitrary fashion. using the Gaussian wave packet as initial state, we find that there are indeed a lot of frequencies in the ZB oscillation.

For some specific parameters, the ZB oscillations in the trapped system are shown in Fig.5. From Fig.5, we can see that, for both the weak and strong spin-orbit coupling, the ZB oscillations display the harmonic oscillatory characteristics within short time interval (20 time unit in Fig.5). This is because when the spin-orbit coupling approaches to zero, the energy-spectrum approach the harmonic oscillator spectrum. In the case of the strong spin-orbit limit, the eigenenergies can be approximated by $E_{m,n} = [-\gamma^2 + 2n + 1 + m^2/\gamma^2]/2$, which is analogous to the energy spectrum formula of two component atoms with strong spin-orbit coupling and harmonic trap [36, 37]. Compared with the two components atoms, the ground state is not degenerate. The energy spectrum in strong spin-orbit coupling limit form landau level-like spectrum. Thus, in cases of both weak and strong spin-orbit coupling limit, the energy level spacing approaches $\hbar\omega$. With the increase of the time, the coherence between oscillations with nearly harmonic frequency gets weaker and weaker. Hence the oscillations with high frequency begin to manifest themselves.

When the spin-orbit coupling strength γ is moderate, the ZB shows quite complicated and irregular characteristics. It is due to the complicated energy spectrum and coexistence of oscillations with various frequencies in ZB.

Recently, the generation of synthetic gauge filed in atoms have been realized experimentally [28–33]. The theoretical proposal to realize spin-orbit coupling in cold

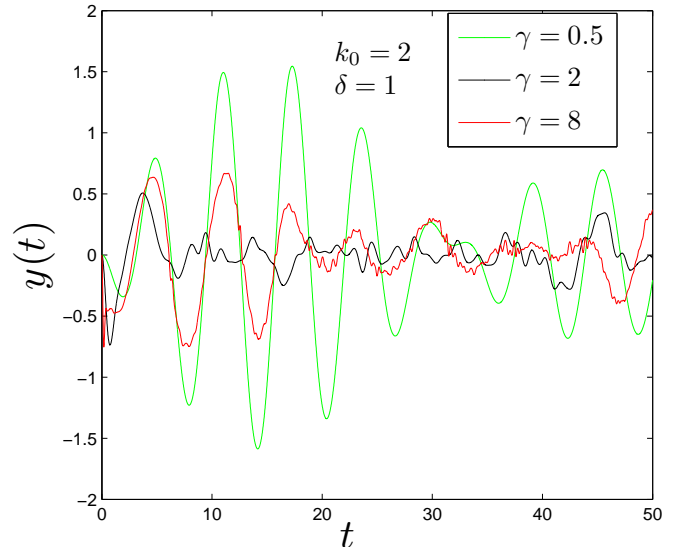


FIG. 5. The ZB oscillations in the trap with an initial Gaussian wave packet for specific parameters (the wave width $\delta = 1$, the average momentum $k_0 = 1$). The green, black and red lines correspond to the specific spin-orbit coupling strength $\gamma = 0.5, 2$ and 8 , respectively.

atoms for three component atoms also have been put forward in Ref. [34]. Using the so-called tetrapod setup scheme, the spin-orbit coupling in spin-1 atoms could be realized in alkali-metal atoms. Compared to the electron, the ZB effect of atoms is detectable by the available experimental techniques. Taking ^{87}Rb atoms for example, one can adopt the typically experimental parameters, such as the wave length of Raman laser $\lambda \sim 800\text{nm}$ can be used, which corresponds the spin-orbit strength $\gamma = \pi\hbar/(m\lambda) = 0.28\text{cm/s}$ ($m = 1.45 \times 10^{-25}\text{kg}$ for ^{87}Rb). The typical size of the wave packet is $\delta \sim 5\mu\text{m}$ in the harmonic trap with frequency $\omega = 2\pi \times 4.6\text{Hz}$.

IV. SUMMARY

In summary, we have investigated the ZB effect in spin-1 atoms in the presence of the Zeeman field and the external parabolic trap respectively. It is shown that the ZB oscillations could be greatly affected by the external Zeeman field and the trap. The applied Zeeman field could suppress or enhance the ZB amplitude and change the frequencies of oscillation. In addition, multi-frequency oscillations could appear in the presence of the Zeeman field. Through adjusting both linear and quadratic Zeeman field properly, we could obtain a much slowly damping ZB oscillation. In the presence of harmonic trap, there would be the ZB oscillation without damping and with arbitrary number of frequencies. By using the Gaussian packet as an initial state, the ZB oscillation in the

trap displays very complicated and irregular characteristics.

The present study may help us understand the role of external Zeeman field and trap in the ZB oscillations in spin-1 atoms. The investigation of effects induced by the external field and trap on ZB oscillation open up new possibilities for manipulation and control of the ZB oscillation. We anticipate the ZB effect be detected in the widely-studied cold atoms experiments with spin-orbit coupling interactions.

Acknowledgements: This work was supported by the NKBRSC under grants Nos. 2011CB921502, 2012CB8213052009CB930701, 2010CB922904, and NSFC under grants Nos. 10934010, 60978019, and NSFC-RGC under grants Nos. 11061160490 and 1386-N-HKU748/10.

Appendix A: The projections of the Gaussian packet onto the harmonic oscillator eigenstates

In this appendix, we give the calculation of the projections of the initial Gaussian wave packet onto the harmonic oscillator basis, which is required in the calculation of the average values of position operator with time. The initial wave packet reads:

$$|g\rangle = \frac{1}{\sqrt{\pi\delta^2}} e^{-\frac{(x^2+y^2)}{2\delta^2}} e^{ik_0x}, \quad (\text{A1})$$

where δ denotes the width of the wave packet and k_0 is the average momentum of wave packet.

The projection onto the harmonic oscillator basis is

$$\langle \phi_{n,m} | g \rangle = \frac{2(-1)^n i^{|m|}}{\delta} \sqrt{\frac{n!}{(n+|m|)!}} \times \int_0^{+\infty} \rho^{|m|+1} e^{-\sigma^2 \rho^2} L_n^{|m|}(\rho^2) J_{|m|}(k_0 \rho) d\rho, \quad (\text{A2})$$

where $|\phi_{n,m}\rangle = R_{n,m}(\rho) \frac{e^{im\theta}}{\sqrt{2\pi}}$, $\sigma^2 = \frac{1}{2}(1 + \frac{1}{\delta^2})$ and $J_{|m|}(x)$ is the Bessel functions of order $|m|$.

The associated Laguerre polynomial consists of various monomials. The integrals corresponding to the monomials can be obtained. We can use the identity

$$\int_0^{+\infty} \rho^{\mu-1} e^{-p\rho^2} J_\nu(a\rho) d\rho = \frac{\Gamma(\frac{\mu+\nu}{2})}{2p^\mu \Gamma(\nu+1)} \left(\frac{a}{2p}\right)^\nu e^{-\frac{a^2}{4p^2}} {}_1F_1\left(\frac{\nu-\mu}{2}+1; \nu+1; \frac{a^2}{4p^2}\right), \quad (\text{A3})$$

where $\Gamma(z)$ is Euler's Gamma function and ${}_1F_1(\alpha; \beta; x)$ is the generalized hypergeometric functions [26]. Combining Eq. (A.3) with Eq. (A3), we can obtain the projections by summing up all integral values corresponding to the monomials. The ZB amplitude operators $\vec{Z}_{k;l}$ in Eq. (15) are also calculated within the harmonic oscillator basis and the mean value of the position operator can be obtained correspondingly.

-
- [1] E. Schrödinger, Sitzungsber. Preuss. Akad. Wiss. Phys. Math. Kl. 24, 418 (1930)
- [2] L. Ferrari and G. Russo, Phys. Rev. B **42**, 7454 (1990).
- [3] T. M. Rusin, and W. Zawadzki, Phys. Rev. B **76**, 195439 (2007).
- [4] T. M. Rusin, and W. Zawadzki, Phys. Rev. B **78**, 125419 (2008).
- [5] T. M. Rusin, and W. Zawadzki, Phys. Rev. B **80**, 045416 (2009).
- [6] J. Schliemann, D. Loss, and R. M. Westervelt, Phys. Rev. Lett. **94**, 206801 (2005).
- [7] J. Cserti and G. Dávid, Phys. Rev. B **74**, 172305 (2006).
- [8] Q. f. Liang, Y. h. Yan, and J. Dong, Optics Letters. **36**, 2513 (2011).
- [9] X. D. Zhang, Phys. Rev. Lett. **100**, 113903 (2008).
- [10] J. Schliemann, New Journal of Physics **10**, 043924 (2008).
- [11] Z. F. Jiang, R. D. Li, Shou-Cheng Zhang, and W. M. Liu, Phys. Rev. B **72**, 045201 (2005).
- [12] S. Q. Shen, Phys. Rev. Lett. **95**, 187203 (2005).
- [13] R. Winkler, U. Zülicke and J. Bolte, Phys. Rev. B **75**, 205314 (2007).
- [14] J. Cserti and G. Dávid, Phys. Rev. B **82**, 201405 (2010).
- [15] M. Lee and C. Bruder, Phys. Rev. B **72**, 045353 (2005).
- [16] Z. Y. Wang and C. D. Xiong, Phys. Rev. A **77**, 045402 (2008).
- [17] Wlodek Zawadzki, Phys. Rev. B **72**, 085217 (2005).
- [18] J. Y. Vaishnav and C. W. Clark, Phys. Rev. Lett. **100**, 153002 (2008).
- [19] Q. Zhang, J. Gong and C. H. Oh, Phys. Rev. A **81**, 023608 (2010).
- [20] J. Larson, J. P. Martikainen and A. Collin, arXiv: 1001.2527v2 (2011).
- [21] D. W. Zhang, Z. D. Wang, S. L. Zhu, arXiv: 1203.5949v1 (2012).
- [22] M. Merkl, F. E. Zimmer, G. Juzeliūnas and P. öhberg, Europhys. Lett. **83**, 54002 (2008).
- [23] G. Dávid, Phys. Rev. B **81**, 121417 (2010).
- [24] B. Ramachandhran, B. Opanchuk, X. J. Liu, H. Pu, P. D. Drummond, and H. Hu, Phys. Rev. A **85**, 023606 (2012).
- [25] Claude Cohen-Tannoudji, Bernard Diu, Frank Lalöe, Quantum Mechanics, Vol. I, (Hermann and John Wiley & Sons, 1977).
- [26] Z. X. Wang and D. R. Guo, Special Functions, (World Scientific, Singapore, 1989).
- [27] V. Ya. Demikhovskii, G. M. Maksimova, and E. V. Frolova, Phys. Rev. B **78**, 115401 (2008).
- [28] Xiong-Jun Liu, Mario F. Borunda, Xin Liu, and Jairo

- Sinova, Phys. Rev. Lett. **102**, 046402 (2009).
- [29] Y.-J. Lin, R. L. Compton, A. R. Perry, W.D. Phillips, J.V. Porto, and I. B. Spielman, Phys. Rev. Lett. **102**, 130401 (2009).
- [30] T. L. Ho and S. Z. Zhang, Phys. Rev. Lett. **107**, 150403 (2011).
- [31] Y. Deng, J. Cheng, H. Jing, C.-P. Sun, and S. Yi, Phys. Rev. Lett. **108**, 125301 (2012).
- [32] D. L. Campbell, G. Juzeliūnas, and I. B. Spielman, arXiv: 1102. 3945v2 (2011).
- [33] Y.-J. Lin, K. Jiménez-García and I. B. Spielman, Nature **471**, 83 (2011).
- [34] G. Juzeliūnas, J. Ruseckas, and J. Dalibard, Phys. Rev. A **81**, 053403 (2010).
- [35] V. Ya. Demikhovskii, G. M. Maksimova, and E. V. Frolova, Phys. Rev. B **81**, 115206 (2010).
- [36] WU Cong-Jun, Ian Mondragon-Shem, ZHOU Xiang-Fa, CHIN. PHYS. LETT. **28**, 097102 (2011).
- [37] H. Hu, B. Ramachandhran, Han Pu, and Xia-Ji Liu, Phys. Rev. Lett. **108**, 010402 (2012).